Effects of the Zeroth Order Diffraction of a Phase Mask on Bragg Grating

Author:
Xiong, Zhengjun; Peng, Gang-Ding; Wu, B; Chu, Pak

Publication details:
Journal of Lightwave Technology
v. 17
Chapter No. 11
pp. 2361-2365
0733-8724 (ISSN)

Publication Date:
1999

Publisher DOI:
http://dx.doi.org/10.1109/50.803031

Effects of the Zeroth-Order Diffraction of a Phase Mask on Bragg Gratings

Z. Xiong, *Member, IEEE,* G. D. Peng, B. Wu, and P. L. Chu

***Abstract*—The effects of the zeroth-order diffraction of a phase mask on the creation of Bragg gratings using the mask technique were theoretically and experimentally investigated. Experimental results showed that the zeroth-order diffraction of 1% total power, while in interference with the first-order diffraction of 44% each, dramatically affected the structure of the gratings in a polymer optical preform, including their period. Theoretical analysis by taking the zeroth-order diffraction into account predicted that a very small part of the zeroth-order component (0.1%) would have substantial effects on the gratings, which will be no longer uniform along both the directions of the incident laser beam propagation and the groove array. Theoretical calculation agrees well with the experimental results.**

***Index Terms*—Diffraction, gratings, interference, optical fiber device fabrication, optical polymers.**

I. Introduction

GRATINGS in optical fiber have become very attractive optical devices and found a wide range of applications in optical fiber communications and sensor systems. Bragg gratings can be fabricated in optical fiber using internal writing [1], the holographic technique [2] and the phase mask technique [3]. The phase mask technique has been widely used in today's fiber grating manufacture due to its superior advantages over the other two techniques [4]. In the phase mask technique, gratings are fabricated by using a phase mask with samples put in near proximity to it. This can greatly simplify the manufacture process, while producing the gratings with a high performance. It also offers easier alignment of the fiber than the holographic does, and relaxes the stability requirements on equipment and elements and the coherence requirements on UV laser beam. In addition, the gratings can be made massively instead of one by one as in the other techniques.

The requirements on the phase mask itself, however, are relatively strict. Normally, most of the diffracted light of a phase mask is contained in the zeroth and the first diffraction orders. For using in Bragg grating writing in optical fiber, the phase mask is designed to suppress the zeroth-order diffraction by controlling the depth of the effective surface relief in the phase mask equal or very close to half of the wavelength of the UV laser beam to be used for grating writing, i.e. $D = \lambda/2(n-1)$. According to scalar theory, the zeroth-order diffraction would be zero in such a designed phase mask. The amount of light in the zeroth order in practice, however, can only be guaranteed at the level of about 1% by the manufacturers, with approximately 40% in each of the two first-order diffraction beams. Furthermore, although the grating period is independent from the writing wavelength, the use of the phase mask is limited at one single writing wavelength. Any change in the UV wavelength away from the specified value will result in the increase in the zeroth-order diffraction with decrease in the first-order intensity.

The investigation into the effects of the zeroth-order diffraction of a phase mask on optical fiber gratings was motivated by the finding that the periods of the gratings were not equal to $\Lambda = D/2$ in our polymer optical preform, if the preform was put directly behind the phase mask [5], where Λ is the period of the gratings and D is the pitch of the phase mask. J. Nishii et al. [6] reported a similar situation where the grating period in a GeO_2-SiO_2 glasses was the same as that of the phase. Both experimental results implied that the period change was not due to the material properties. It is a general problem with the phase mask technique due to the zeroth-order effects [7], [8]. In this paper, we report our experimental results, followed by the theoretical analysis and discussion.

II. Experimental Results

The experimental setup is schematically shown in Fig. 1. The UV laser beam was the output of a frequency-doubled optical parametric oscillator (OPO), which was pumped by a frequency-tripled Nd:YAG pulse laser. The wavelength used in this experiment was 248 nm, at which the OPO was adjusted to have a pulse energy of 5 mJ, pulse width of 5 ns and repetition rate of 10 Hz. The preparation of the Bragg gratings in the polymer preforms was carried out by exposing the preforms to the UV laser beam through a fused silicon phase mask, which has a one-dimensional surface relief pattern. The dimension is 3 mm by 10 mm and the period is 1.0614 μm. The diffraction efficiency of the two first orders is 44% each and the zeroth-order diffraction was suppressed to about 1% for 248 nm writing wavelength. The sample was cut from a polymer optical preform, that is sensitive to the UV laser [5], [9], and exposed to the laser for about 90 seconds.

We detected the diffraction from the preform grating using an Argon laser with operation wavelength of 488 nm. The measured value of the first-order diffraction angle was about

Manuscript received February 16, 1999; revised July 23, 1999. This work was supported by the Australian Photonics Cooperative Research Centre and Australian Research Council.

Z. Xiong was with the Optical Communications Group, School of Electrical Engineering, The University of New South Wales, Sydney 2052 Australia. He is now with the Gintic Institute of Manufacturing Technology, Singapore 638075 Singapore.

G. D. Peng, B. Wu, and P. L. Chu are with the Optical Communications Group, School of Electrical Engineering, The University of New South Wales, Sydney 2052 Australia.

Publisher Item Identifier S 0733-8724(99)08932-X.

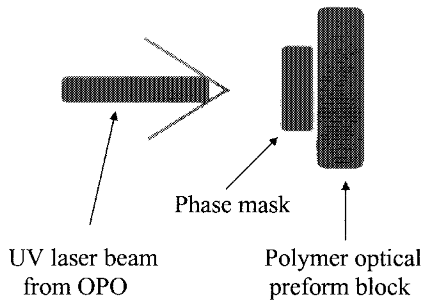

Fig. 1. Experimental setup for grating writing. The preform was put behind and in touch with the output plane of the phase mask.

27.3°, corresponding to a grating pitch of 1.06 μm, which was very close to the value of the phase mask period. This result was surprising, because the expected period was nearly doubled. To confirm this result, we used an atomic force microscope (AFM) to characterize the gratings. Fig. 2 is the AFM photo for the grating written at 248 nm. It is revealed that the grating was produced mainly by periodically removing the polymer's surface, and its period was 1.06 μm. It is also observed that the removal is not sinusoidal. Fig. 3 is the AFM section analysis profile of the grating, which shows the surface relief distribution along the cross section of the grating. Note that the profile includes two sets of oscillations. One is deeper and the other is more shallow, each has a period of about 1.06 μm, as indicated by the two dark arrows shown in the figure. For convenience, we may denote the deeper one as grating I and the other grating II. Grating II locates approximately a half period away from grating I. We should also note here that the relief depth measured by AFM did not reflect its real value due to the limit of AFM and the grating distortion. This is explained in the following.

Careful observation inside the gratings was also performed under an optical microscope. Using a 100× objective lens with the microscope, we could see grating I not only on the surface, but also inside the sample by changing the focus point of the microscope. The observation revealed that the gratings have a thickness more than 10 μm other than the value shown in Fig. 3, but are not uniform along the depth direction. This indicated that they were not straightforward and have been distorted in the depth direction. It is also observed the gratings were divided into layers in this direction and the distance between layers was measured to be about 8.5 μm. Each layer has a grating with the same period of 1.06 μm and between layers there is a shift of about 0.5 μm in the cross-section direction. We failed to observe grating II under the optical microscope due to its low contrast and dimness.

All these results presented above indicated that the grating created by the phase mask technique was no longer of the characteristics as predicted by the two beams interference theory. It needs to consider the effects of other diffraction orders besides the first orders, particularly the zeroth order.

III. Theoretical Analysis

Fig. 4 shows the coordinate system used for the following analysis. The z direction denotes the laser beam incident direction on the phase mask and the x direction the grooves array direction. The original point O is chosen in the output plane of the phase mask. The phase change behind the phase mask at position (xz) in respect to point O is $2\pi S_N/\lambda$ for the Nth-order diffraction where $S_N = x\sin(\theta_N) + z\cos(\theta_N)$, θ_N is the diffraction angle of the Nth-order with $\sin(\theta_N) = N\lambda/D$ where D is the period of the phase mask.

The electrical field distribution behind the phase mask is

$$E = \sum_{k=-N}^{N} C_k \exp(i2\pi S_k/\lambda) \tag{1}$$

where C_k is the amplitude of the electrical field of the kth-order diffraction. Here we only consider the symmetrical diffraction situation where $C_k = C_{-k}$, and replace the zeroth-order amplitude with $2C_0$. The intensity EE^* distribution is then

$$\begin{aligned} I = 4\Bigg\{\sum_{k=0}^{N}\Bigg[&C_k^2\cos^2(2k\pi x/D) \\ &+ \sum_{j\neq k} C_k C_j \cos(2k\pi x/D)\cos(2j\pi x/D) \\ &\times \cos(2\pi z(\cos\theta_k - \cos\theta_j))/\lambda\Bigg]\Bigg\}. \end{aligned} \tag{2}$$

To simplify our discussion in the following, the diffraction orders higher than ± 1 will be ignored. For the normal interference pattern of the two first-order diffraction beams, the intensity distribution is

$$I_{\pm 1} = 4C_1^2\cos^2(2\pi x/D) \tag{3}$$

which demonstrates that the fringe pattern is similar to the structure of the phase mask, that is, the pattern has uniform intensity along both the directions of the zeroth-order beam propagation (z direction) and the grooves of the phase mask (y direction). The difference is that it has a sinusoidal distribution along the cross-section direction (x direction) with a period equal to half of the phase mask's period.

If we take the zeroth-order diffraction into account, the distribution changes to

$$\begin{aligned} I_{0,\pm 1} = 4\big[&C_1^2\cos^2(2\pi x/D) + C_0^2 + 2C_0C_1\cos(2\pi x/D) \\ &\times \cos(2\pi z(1-\sqrt{1-(\lambda/D)^2})/\lambda)\big]. \end{aligned} \tag{4}$$

In the right side of (4) three terms are included. The first term is the same as (3), i.e., the interference of the two first-order beams. The second term, $4C_0^2$, is a constant, coming from the zeroth-order diffraction, which reduces the contrast of the fringe pattern of the first term. The third term is due to the interaction between the zeroth order and the two first-order diffraction beams. It changes along both x and z directions. For a fixed z value, this term also predicts a sinusoidal distribution along the cross-section direction as (3) does, but with a different period, which is exactly equal to the period of the phase mask. Its intensity is dependent on the intensity of the zeroth order and the first-order diffraction and the position

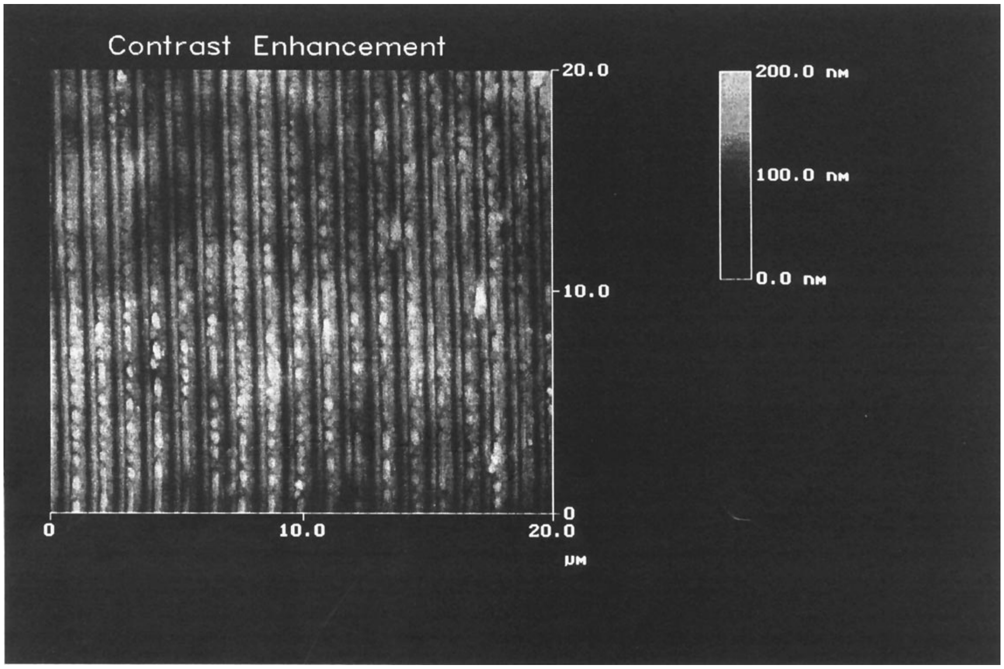

Fig. 2. An AFM photograph showing the structure of the surface relief grating in a polymer optical preform.

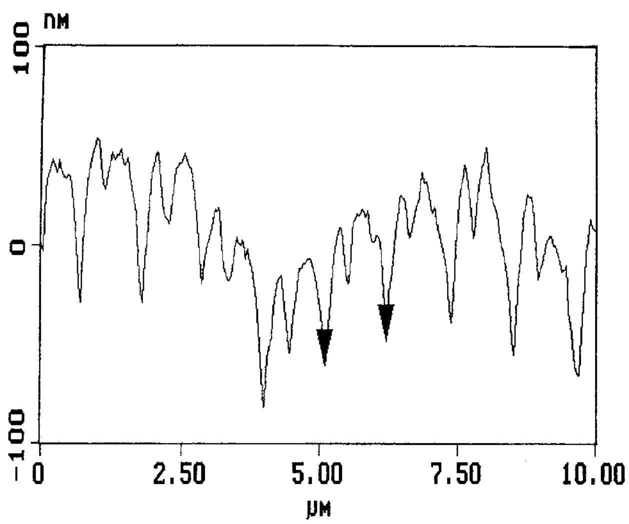

Fig. 3. The cross-section analysis profile of the grating shown in Fig. 2. The vertical axis stands for the depth of the surface relief. Note that due to the AFM limits and the properties of the grating described in the text, the depth of the relief is much larger than the values shown in this figure.

in the z direction. At a fixed position in the x direction, the distribution is also sinusoidal but with a period

$$z_0 = \lambda/(1 - \sqrt{1-(\lambda/D)^2}). \tag{5}$$

To compare the theoretical calculation of (4) and (5) with the experimental results presented in the pervious section, we set all the values of the parameters in the equations as those used in the experiments. That is, $\lambda = 248$ nm, $D = 1.0614$ μm, $(2C_0)^2 = 1\%$ and $C_1^2 = 44\%$. In this case, the period of the sinusoidal change in intensity distribution in the z direction is $z_0 = 8.96$ μm, which agrees well with the experimental value of 8.5 μm, with an experimental error of about 5%.

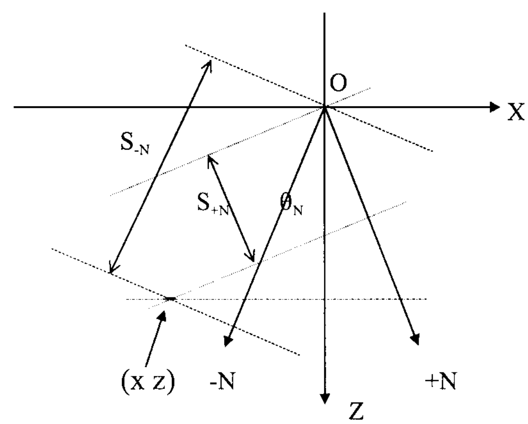

Fig. 4. The coordinate system to simulate the three beams interference. X is the direction of the groove array and Z is the direction of the incident laser propagation, which is the same as the normal of the phase mask.

The intensity distributions for different levels of the zeroth-order diffraction in the plane of the phase mask output surface are calculated as shown in Fig. 5, where the horizontal axis presents the distance in the cross-section direction (the X axis in Fig. 4). The pattern of the curve in Fig. 5(a), corresponding to a zeroth-order diffraction level of 1%, consists of two sets of pulse sequences, each with the same period of 1.06 μm as that of the phase mask, but with a different amplitude value. To simplify, we call them as grating 1 and grating 2 as marked in the figure. The distance between grating 1 and 2 is equal to $D/2$ (0.53 μm) in the cross-section direction. These are reminiscent of the AFM curve in Fig. 3, which has all the features of Fig. 5(a). Fig. 5(b)–(e) depict another four curves with different intensity levels of the zeroth-order diffraction. It can be seen that as the zeroth-order intensity decreases from $(2C_0)^2 = 10\%$ to 0, the interference distribution gradually becomes a uniform periodic structure with a pitch value of

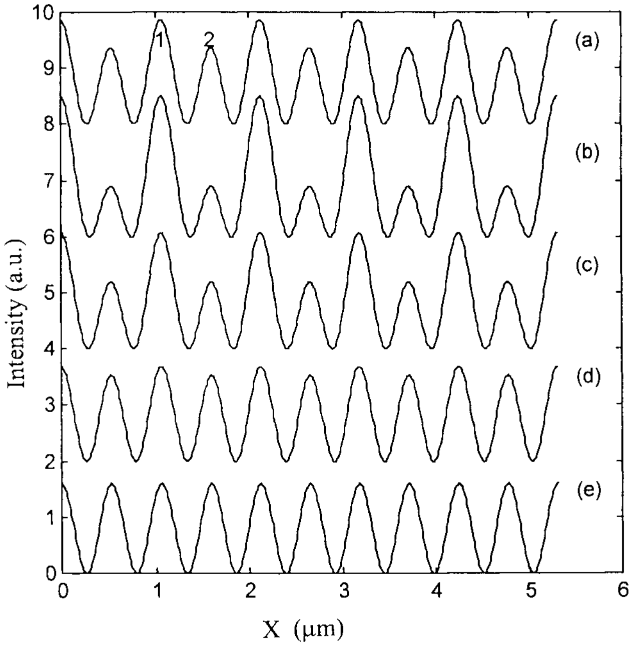

Fig. 5. The interference distribution along the x direction at $z = 0$ with different levels of the zeroth-order diffraction $(2C_0)^2$: (a) 1%; (b) 10%; (c) 3%; (d) 0.1%; and (e) 0%.

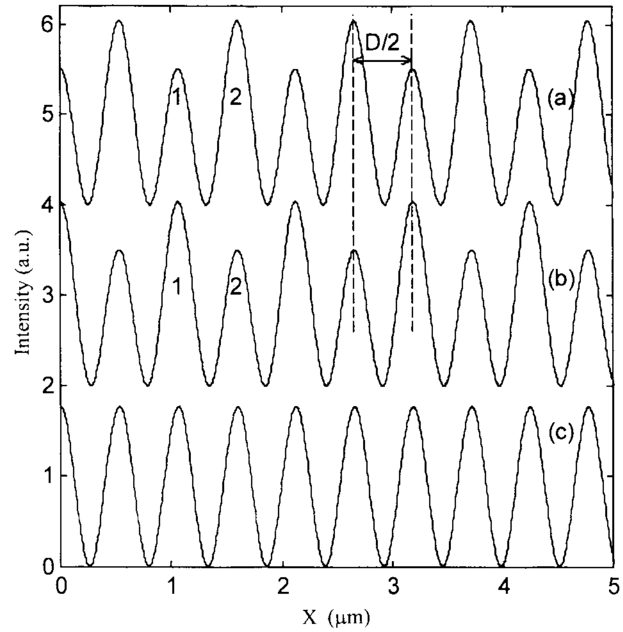

Fig. 6. The interference distribution for $(2C_0)^2 = 1\%$ and $C_1^2 = 44\%$ along the x direction at different z positions: (a) $z = z_0/2$ (4.98 μm), (b) $z = 0$, and (c) $z = z_0/4$ (2.49 μm).

0.53 μm as shown in Fig. 5(e) where $C_0 = 0$, corresponding to the usual interference fringe pattern of the two first-order laser beams. Therefore, we can conclude that the emergence of grating I and II in Fig. 3, or grating 1 and 2 in Fig. 5, is mainly due to the intrusion of the zeroth-order diffraction.

The extent of the zeroth-order effects on the gratings can be estimated with (4). At $z = 0$, the intensity peak values of grating 1 and 2 are $4(C_1 + C_0)^2$ and $4(C_1 - C_0)^2$, respectively. The peak intensity change from grating 1 to 2 is then $4C_1C_0/(C_1 + C_0)^2$. Under our experimental conditions, the change is 27%, while for a level of $(2C_0)^2 = 0.1\%$, the case in Fig. 5(d), it is ~10%. Thus, the effects of the zeroth order is substantial even it is very small.

Fig. 6 is the calculated distributions of the diffraction intensity for $(2C_0)^2 = 1\%$ and $C_1^2 = 44\%$ at: (a) $z = z_0/2$ (=4.98 μm); (b) $z = 0$ and (c) $z = z_0/4$ (=2.49 μm) behind the phase mask. As z varies, the amplitudes of the two pulse sequences change according to (4). The fringe pattern at $z_0/2$ [as shown in Fig. 6(a)] has a maximum shift in the cross-section direction in respect to the fringe pattern in the phase mask output plane [$z = 0$ as shown Fig. 6(b)]. Both curves (a) and (b) have the same features as discussed in the previous paragraph and the shift in respect to each other is exactly equal to 0.53 μm, half of the phase mask's period. Note that at $z = 0$, grating 1 has a maximum value and grating 2 a minimum, while grating 1 becomes minimum and grating maximum at $z = z_0/4$. Fig. 6(c) shows the case where grating 1 and grating 2 become equal to form a uniform grating. A comprehensive diffraction distribution can be clearly seen in a 3-D figure as shown in Fig. 7.

We should note here that the simplified analysis presented above by ignoring the higher orders does not have a significant impact on its generality. The reasons are given as follows. The

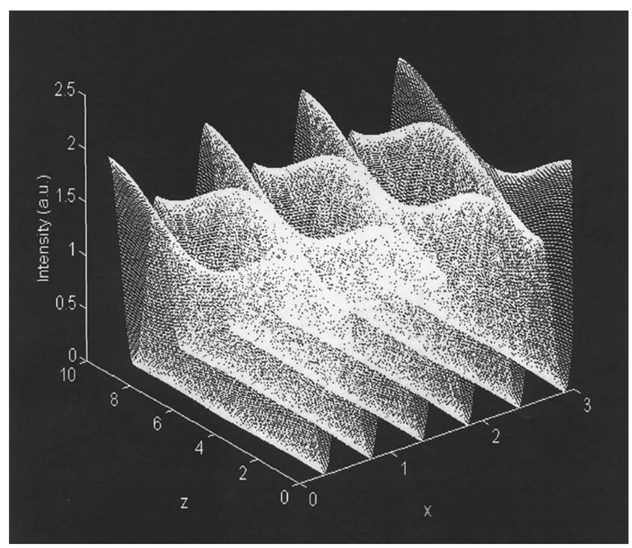

Fig. 7. The three dimensional intensity distribution of the three beams interference [see (4)] with experimental parameters: $\lambda = 248$ nm, $D = 1.0614$ μm, $(2C_0)^2 = 1\%$, and $C_1^2 = 44\%$.

simulation results show that the even diffraction orders, while interacting with the first diffraction orders, change the period of the interference pattern, thus the grating pitch, in the same way as that of the zero order, but with much smaller extent as their intensities are much weaker. The higher odd diffraction orders, while interferring with the first diffraction orders, can enhance the effect of normal grating formation. This is because the interference pattern between the first orders and the higher odd orders has the same period as that formed by the two first orders. In this case, however, the intensity distribution is not longer sinosoidal as predicted by (3). This agrees well with the AMF photo. The interactions between the zeroth order and the higher orders is more complicated, but their influence on the grating formation is at least one order smaller than that of the zeroth order.

All the distributions shown in Figs. 5 to 7 unambiguously predict that the introduction of the zeroth-order diffraction by the phase mask into the interference destroys the quality of the Bragg gratings. Its effects are substantial even the zeroth-order intensity is as small as 0.1%. Therefore, it is essential that the zeroth-order diffraction is completely eliminated in making high quality fiber gratings.

In order to overcome the effects of the zeroth-order diffraction on the grating writing in optical fibers, the usual way is to modify the setup configuration as given in [10], where only the two beams of the first order diffraction participate in the interference, while the zeroth-order diffraction is blocked. In this case, because the beams form a modified Sagnac optical ring where the counter-propagating beams travel nearly the same optical path, the feature of lower coherence requirements on the ultraviolet (UV) laser beam remains. In addition, it can also overcome the drawback of the phase mask technique. By shifting the intersecting point in the incident plane, the interference angle can be increased or decreased. In turn, the Bragg wavelength can be tuned in a large range. Therefore, a large amount of gratings with different periods can be made using only one phase mask. This will dramatically reduce the manufacture cost.

IV. Conclusion

We have reported that surface relief gratings in a polymer optical preform, created by 248 nm UV laser using the phase mask technique, were affected due to the participation of the zeroth-order diffraction of the phase mask in the formation of the interference fringe pattern of the UV laser beams. The effects of the zeroth-order diffraction were simulated by calculating the fringe pattern of three beams interference behind the phase mask. Theoretical calculation agreed well with our experimental results. Both theoretical and experimental results suggested that the effects of the zeroth-order existence in the interference are detrimental to the quality of the Bragg gratings, including the change in grating's period and nonuniform distribution of the structure. The effects are considerable even the intensity of the zeroth order is much smaller than that of the first orders. In order to obtain high performance Bragg fiber gratings, it is therefore suggested to modify the present phase mask technique by using a modified Sagnac optical ring.

Acknowledgment

The authors would like to thank T. Whitbread for useful discussion.

References

[1] K. O. Hill, Y. Fujii, D. C. Johnson, and B. S. Kawasaki, "Photosensitivity in optical fiber waveguides: Application to reflection filter fabrication," *Appl. Phys. Lett.*, vol. 32, pp. 647–649, 1978.
[2] G. Meltz, W. W. Morey, and W. H. Glenn, "Formation of Bragg gratings in optical fibers by a transverse holographic method," *Opt. Lett.*, vol. 14, pp. 823–825, 1989.
[3] K. O. Hill, B. Malo, F. Bilodeau, D. C. Johnson, and J. Albert, "Bragg gratings fabricated in monomode photosensitive optical fiber by UV exposure through a phase mask," *Appl. Phys. Lett.*, vol. 62, pp. 1035–1037, 1993.
[4] K. O. Hill and G. Meltz, "Fiber Bragg grating technology: Fundamentals and overview," *J. Lightwave Technol.*, vol. 15, pp. 1263–1276, 1997.
[5] G. D. Peng, Z. Xiong, and P. L. Chu, "Photosensitivity and gratings in dye-doped polymer optical fibers," *J. Optic. Fiber Tech.*, vol. 5, pp. 242–251, 1999.
[6] J. Nishii, H. Yamanaka, H. Hosono, and H. Kawazoe, "Preparation of Bragg gratings in sputter-deposited GeO_2-SiO_2 glasses by excimer-laser irradiation," *Opt. Lett.*, vol. 21, pp. 1360–1362, 1996.
[7] J. D. Prohaska, E. Snitze, and J. Winthrop, "Theoretical description of fiber Bragg reflectors prepared by Fresnel diffraction images," *Appl. Opt.*, vol. 31, pp. 3896–3900, 1994.
[8] Z. S. Hegedus, "Contact printing of Bragg gratings in optical fibers: Rigorous diffraction analysis," *Appl. Opt.*, vol. 36, pp. 247–252, 1997.
[9] Z. Xiong, G. D. Peng, B. Wu, and P. L. Chu, "Highly tunable Bragg gratings in single mode polymer optical fibers," *IEEE Photon. Technol. Lett.*, vol. 11, pp. 352–354, 1999.
[10] J. L. Archambault, L. Reekie, and P. St. J. Russell, "100% reflectivity Bragg reflectors in optical fibers by single excimer laser pulses," *Electron. Lett.*, vol. 29, pp. 453–455, 1993.

Z. Xiong (M'98), photograph and biography not available at the time of publication.

G. D. Peng, photograph and biography not available at the time of publication.

B. Wu, photograph and biography not available at the time of publication.

P. L. Chu, photograph and biography not available at the time of publication.